

## NUMERICAL SIMULATION OF TRANSIENT FLOW HEAT TRANSFER IN SUPER CRITICAL CO<sub>2</sub> PIPELINE: FINITE ELEMENT APPROACH

*M. Koolivand- Salooki<sup>1</sup>, S. J. Poormohammadian<sup>2</sup>, A. Azarmehr<sup>3\*</sup>, H. Karimi<sup>4</sup>, J. Sadeghzadeh Ahari<sup>5</sup>*

<sup>1</sup> Gas Research Division, Research Institute of Petroleum Industry (RIPI), Tehran, Iran

<sup>2</sup> Chemical Engineering Department, Yasuj University, Yasuj, Iran

<sup>3</sup> Bidboland Gas Refining Company, Omidyieh, Khuzestan, Iran

<sup>4</sup> Chemical Engineering Department, Yasuj University, Yasuj, Iran

<sup>5</sup> Gas Research Division, Research Institute of Petroleum Industry (RIPI), P.O. Box: 14665-137, Tehran, Iran

Received February 6, 2017; Accepted April 27, 2017

---

### Abstract

An optimized CO<sub>2</sub> pipeline transport system is necessary for large-scale carbon capture and sequestration (CCS) and also CO<sub>2</sub> injection plant (Enhanced oil recovery) implementation. In this research, a CO<sub>2</sub> pipeline buried underground was numerically analyzed, and the hydrodynamic performances of CO<sub>2</sub> pipeline as well as the impacts of multiple factors on pressure drop behavior along the pipeline were studied. Additionally, the thermal behavior of CO<sub>2</sub> pipeline under harsh climate of Iran was investigated. The simulation results exhibit that pipe diameter, and soil temperature affect both the pressure drop and heat transfer behavior of the fluid. The influence of the soil thermal property affects the temperature of the pipe wall. The pipe diameter controls the pressure drop and influences significantly the required output thermal power needed to maintain the favored pipe wall temperature. Furthermore, the burial depth of the pipeline is very critical for distribution of the surrounding temperature above the pipeline. The design of pipeline system, insulation type, insulation size were optimized to achieve a lowest CO<sub>2</sub> temperature variation along the pipeline length.

**Keywords:** Heat transfer; CO<sub>2</sub> pipeline; numerical simulation; CFD; solid medium.

---

## 1. Introduction

Supercritical fluids are widely used in various industries such as power engineering, aerospace engineering, chemical engineering, cryogenics, and refrigeration engineering. In the supercritical region, small temperature and pressure changes can lead to significant changes in the thermo-physical properties of the fluid [1-3]. Convection and conduction heat transfer of fluids at supercritical pressures have many special features due to the sharp variations of the thermo-physical properties. The buoyancy forces stemming from the non-uniform density distribution across the cross section and acceleration or deceleration of the flow due to expansion or contraction of the fluid are the result of significant axial variations of the bulk temperature with heating and cooling alike [4-8]. CO<sub>2</sub> is one of the compounds that can be employed in supercritical state in various industrial applications. CO<sub>2</sub> compression and transportation issues have a long tradition in modern industrial processes. They are gaining importance in the current worldwide discussion of the global climate change. Anthropogenic carbon dioxide emissions arise mainly from combustion of fossil fuels [9] and biomass in power generation, air-blown gasification [10], industrial processes such as cement production [11], natural gas processing, hydrogen production and petroleum refining [12], building and transport sectors. The CO<sub>2</sub> capture and storage chain are subdivided into four systems: the system of capture and compression, the transport system, the injection system and the storage system.

Among the several approaches to transport CO<sub>2</sub>, pipeline transportation is the most economical method to transport large amounts of CO<sub>2</sub> for long distances [13-14]. Normally, it is recommended that the pipeline should be operated at high pressure (usually higher than the critical pressure of CO<sub>2</sub>) to increase the transport capability and reduce capital cost of the pipeline system [15-16]. The temperature profile of the CO<sub>2</sub> flow along the pipeline is entangled with the profile of pressure drop. Due to the heat dissipation rates from pipelines, heat transfer of hot fluid to the surrounding environment, thermal insulation may be complemented with integrated heating systems to lessen heat loss from the fluid. Thermal designs such as thermal insulation, direct electrical heating techniques [17] and pipe-in-pipe systems have been employed to maintain the temperature of fluids being transported efficiently. Burial pipeline reduces the risk resulting from axial thermal expansion [18]. In comparison with pipe-in-pipe thermally-insulated systems, this method illustrates a cost effective thermal insulation.

Zhang *et al.* [19] studied the pressure drop behavior of supercritical CO<sub>2</sub> along the pipeline using ASPEN Plus software. They studied pressure drops and maximum safe transport distance along the pipeline. They were unable to simulate the temperature differences between the CO<sub>2</sub> and environment precisely because of the limitation of ASPEN Plus software. McCoy and Rubin [20] applied a one-dimensional model of CO<sub>2</sub> flow along the pipeline, but they assumed the flow temperature of CO<sub>2</sub> in the pipeline was always constant as the environmental temperature which is not a correct assumption.

In the present study, we studied the thermal behavior of CO<sub>2</sub> transport along the insulated pipeline numerically based on finite element method (FEM). In this method, we considered the influences of multiple factors encompassing insulation, heat conduction between the CO<sub>2</sub> and environment and environmental temperature, so the thermal behavior of real flow transport process can be simulated more accurately.

## 2. Material and methods

In the process of designing CO<sub>2</sub> transportation pipeline, the most important problem is to find the maximum safe transport distance. For longer transport distances, a boosting compressor station should be introduced to maintain the pressure value above 160 bar. At a given inlet pressure, the safe transportation distance depends strongly on ambient temperature. An increase in ambient temperature reduces CO<sub>2</sub> density and increases the velocity along the pipeline increasing the pressure drop and leading to build up choking conditions. A bigger pressure drop means higher operating costs and possibly considering recompression stations. Hence, any optimization of CO<sub>2</sub> transport via a pipeline must take the impact of ambient temperature into account because of heat exchanged between CO<sub>2</sub> in the pipe and the surroundings along the pipeline. In designing a pipeline, the extreme case with the highest environmental temperature should be taken into consideration to ensure that the pipeline can work well all through the year. For our study, the maximum value of ambient (soil) temperature in the south of Iran has been considered. These temperature values are 30°C in the summer and 15°C in the winter.

### 2.1. CO<sub>2</sub> phase behavior

The properties of CO<sub>2</sub> clarified why the working state for CO<sub>2</sub> transport should be either in liquid or supercritical state. Figure 1 shows the phase diagram of CO<sub>2</sub>, from which it can be seen that the critical temperature and pressure of CO<sub>2</sub> are 30.98°C and 7.38 MPa, respectively. When CO<sub>2</sub> becomes a super-critical fluid, it will have a relatively large density, good compressibility, and small viscosity. Due to higher critical temperature of CO<sub>2</sub> than normal soil temperature, insulation measurements are required to maintain CO<sub>2</sub> at supercritical state, or it should be heated after a certain distance. Although Zhang *et al.* [19] proposed that transporting liquid CO<sub>2</sub> at relatively low temperature is preferred to reduce pressure drop along the pipeline, some studies proposed that CO<sub>2</sub> should be transported in supercritical phase [13,21]. In this study, CO<sub>2</sub> transport was considered in supercritical state.

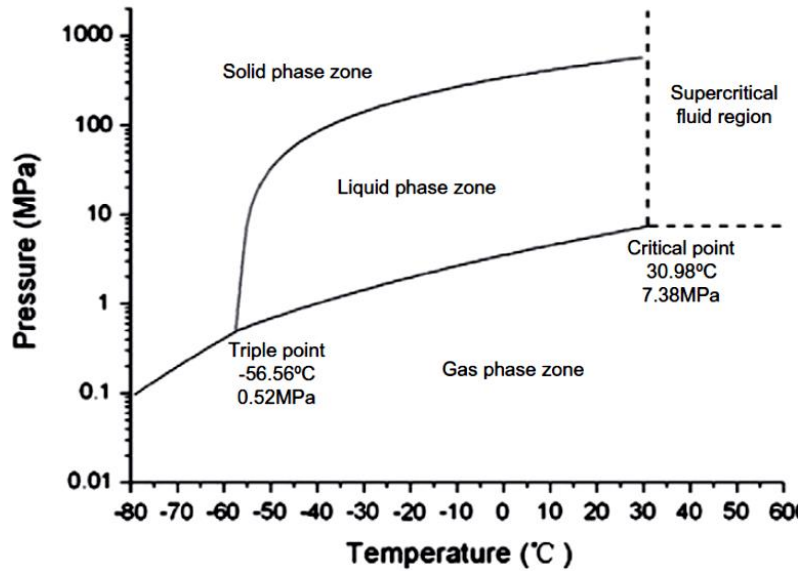


Figure 1 Phase diagram of pure CO<sub>2</sub> (the top-right area is the supercritical area) [10]

## 2.2. Non-isothermal transient flow formulation

From the laws of conservation of mass, momentum, and energy, the basic equations regarding partial differential equations describing a one-dimensional transient single phase compressible flow may be expressed as follows [22]:

$$\frac{\partial p}{\partial t} + v \frac{\partial p}{\partial x} + \rho a_s^2 \frac{\partial v}{\partial x} = \frac{a_s^2}{c_p T} \left( 1 + \frac{T}{z} \left( \frac{\partial z}{\partial T} \right)_p \right) \left( \frac{q + wv}{A} \right) \quad (1)$$

$$\frac{\partial v}{\partial t} + v \frac{\partial v}{\partial x} + \frac{1}{\rho} \frac{\partial p}{\partial x} = -\frac{W}{A\rho} - g \sin \theta \quad (2)$$

$$\frac{\partial T}{\partial t} + v \frac{\partial T}{\partial x} + \frac{a_s^2}{c_p} \left( 1 + \frac{T}{z} \left( \frac{\partial z}{\partial T} \right)_p \right) \frac{\partial v}{\partial x} = \frac{a_s^2}{c_p p} \left( 1 - \frac{p}{z} \left( \frac{\partial z}{\partial p} \right)_T \right) \left( \frac{q + wv}{A} \right) \quad (3)$$

where  $a_s$  is the isentropic wave speed defined as:

$$a_s^2 = \frac{zR_sT}{\left[ 1 - \frac{p}{z} \left( \frac{\partial z}{\partial p} \right)_T - \frac{p}{\rho c_p T} \left( 1 - \left( \frac{T}{z} \right) \left( \frac{\partial z}{\partial T} \right)_p \right)^2 \right]} \quad (4)$$

and the frictional force per unit length is given by:

$$w = \frac{f\rho v|v|}{8} \pi D \quad (5)$$

The friction factor,  $f$ , is calculated from the Colebrook–White equation [23]:

$$\frac{1}{f} = -2 \log \left( \frac{\varepsilon}{3.7d} + \frac{2.51}{Re\sqrt{f}} \right) \quad (6)$$

The heat transfer rate of the fluid to the surroundings per unit length is defined as follows:

$$q = -\pi DU(T - T_s) \quad (7)$$

The overall heat-transfer coefficient for a completely buried pipeline is calculated from the equation 8. In order to have safe operations, pipelines are often buried at a depth of 1.2-1.5 m, ensuring more stable temperatures than that on the surface. Finite element meshes of the two-layer model are shown in Figs. 2 and 3.

$$U = \frac{1}{\left( \frac{r_1}{k_{in}} \ln \left( \frac{r_2}{r_1} \right) + \left( \frac{r_1}{k_{soil}} \right) \ln \left( \frac{z}{r_2} \right) + \left( \frac{r_1}{z} \right) \left( \frac{1}{h_g} \right) \right)} \quad (8)$$

Insulated and buried pipelines provide more thermal resistance. Therefore, the convective heat transfer from the CO<sub>2</sub> and heat resistance from the steel pipeline wall can be neglected. The heat conductivity is 25 W/(mK), and 0.058 W/(mK) for the pipe wall material and insulation layer material, respectively. The thermal conductivity of the soil is assumed to be 1.21 W/(mK), and the distance between the ground surface and the pipe center is 1.225 m. The air convection heat transfer coefficient is 5 W/(m<sup>2</sup>K).

According to [13, 21, 24], the thermal resistance of the convective heat transfer between the CO<sub>2</sub> and the inner pipe wall is much smaller than that of the pipe wall and the heat insulation layer, so it is assumed that the temperature of the inner pipe wall is equal to the temperature of CO<sub>2</sub> at the same cross section. The calculated heat transfer coefficient  $k$  between the ground and CO<sub>2</sub> for pipelines with 0.06 m and 0.04 m heat insulation is 0.8524 and 0.985 W/(m<sup>2</sup>K), respectively. This coefficient for a pipeline without insulation is 2.86 W/(m<sup>2</sup>K).

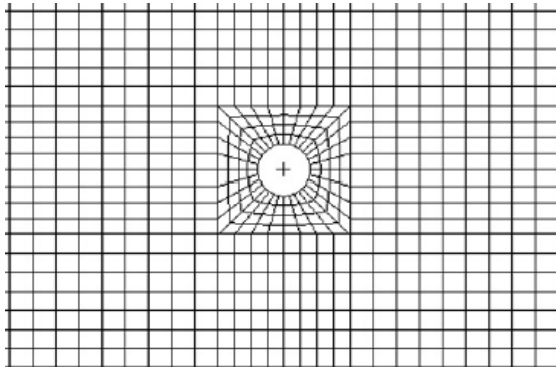


Figure 2 Finite element mesh of the two layers model

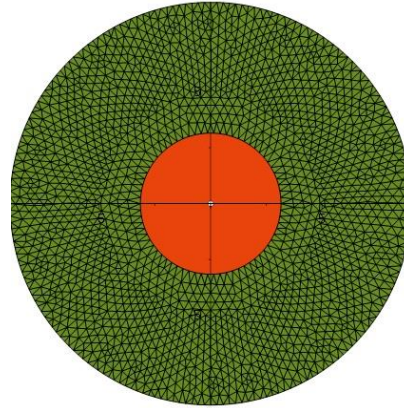


Figure 3 Meshed simulation geometry in finite element analysis

### 2.3. Theory

Finite element is a suitable tool which can simulate the heat transfer in pipelines by numerical computation. It can predict the transient thermal behavior of the surrounding soil. Thus, the model is very useful for the surroundings of a pipe that cannot be assumed as a constant thermal reservoir.

By finite element calculations, the following equations were solved in two steps: 1. Energy equation for the fluid in the pipe and 2. Heat transfer equations for the pipe wall layers. These equations are solved for each of the pipe sections along the pipelines, giving the profiles of the fluid temperature along the pipeline and in the pipe wall. The finite element model establishes the thermal coupling of the pipelines and solves the two-dimensional heat transfer equation in the solid medium surrounding the pipe wall, giving the temperature distribution over the cross sections as well as the interaction between fluid temperatures in embedded pipes. The combination of 1-dimensional fluid and wall temperature equations along the pipelines and the 2-dimensional heat transfer equation for the media in each of the cross sections along the pipeline results a 3-dimensional temperature profile. For an incompressible fluid in the pipe, the governing equations for this system are:

$$\rho^f C_p^f A^f \frac{\partial T^f}{\partial t} = -\dot{m} C_p^f \frac{\partial T^f}{\partial z} - \dot{Q}_{WALL} \quad (9)$$

$$\rho^w C_p^w A^w \frac{\partial T^w}{\partial t} = +\dot{Q}_{WALL} - \dot{Q}_{FEM} \quad (10)$$

$$\rho C_p \frac{\partial T}{\partial t} = \frac{\partial}{\partial x} \left( \lambda \frac{\partial T}{\partial x} \right) + \frac{\partial}{\partial y} \left( \lambda \frac{\partial T}{\partial y} \right) \quad \lambda \vec{q} = -\vec{\nabla} T \quad (11)$$

In addition, a set of boundary and initial conditions is required for the calculation. The temperature  $T = T(x, y, z, t)$  is the key variable. The parameters in the model are listed in the nomenclatures.

Fluid temperature varies only in the axial ( $z$ ) direction. The heat conduction in the first wall layer, therefore, is always in the radial ( $r$ ) direction. The temperature of the fluid and the temperature of the pipe wall were solved with the OLG model (finite difference method) on the assumption that radial heat conduction is predominant. Thus, the pipe wall outer surface serves as an external boundary to the finite element equation. The heat conduction in the rest

of the cross section is in two spatial directions (x and y). It is feasible to include more than one radial conduction wall layer in the model.

One needs to determine the number of nodes required to obtain a suitable grid and time step to obtain numerical solutions to the heat transfer equation. The numerical accuracy is strongly dependent on the number of internal nodes (N) between external boundaries.

### 3. Results and discussion

At the ground surface, either a constant temperature or a constant heat transfer coefficient is usually assumed as a boundary condition. Commonly, pure heat conduction in the soil is taken into account, i.e. combined heat and water transfer is ignored. For homogeneous conditions, the material properties (pipe, insulation, and soil) are assumed to be isotropic, and phase changes are not considered. In order to consider convection as well as radiation, a constant heat transfer coefficient ( $14.6 \text{ W}/(\text{m}^2 \text{ K})$ ) was assumed for the ground surface [25].

Time dependent undisturbed ground temperature was also used for the bottom of the domain. The symmetry condition was used at the left and the right sides. By taking the supply and return temperatures for the inside section of the pipe walls as boundary conditions, the heat loss can be evaluated by heat conduction. The cross section of the simulation geometry is illustrated in Figures 4 and 5.

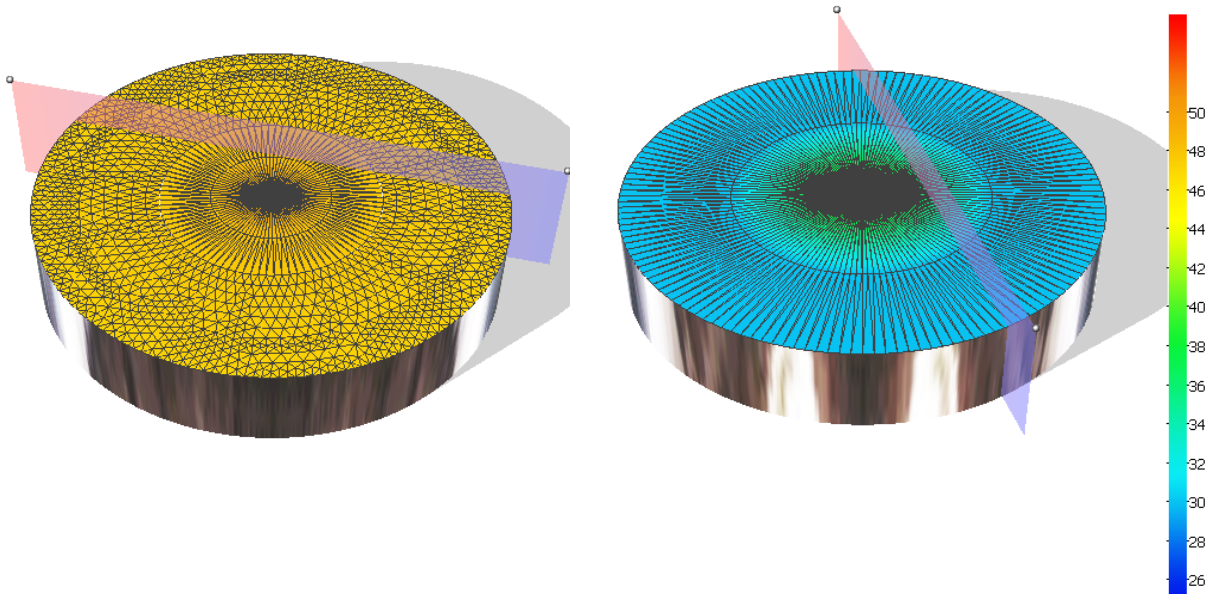


Figure 4 3D meshed simulation geometry

Figure 5 Temperature profile plotted by finite element analysis with insulation; summer case [Centigrade]

#### 3.1. Finite element analysis of CO<sub>2</sub> pipeline

Transient numerical simulation of the temperature field around the buried heating pipeline was run for the chosen values of soil heat conductivity coefficient of  $1.2 \text{ W}/(\text{m}^2 \text{ K})$ . In transient simulations, in addition to the impact of environmental temperature, the influences of other hydraulic parameters were also taken into account.

Experimental works are expensive to perform and are time-consuming. Sometimes there are risks and environmental issues involved in designing these test facilities, so it is necessary to investigate the stability of buried pipeline using a computer modeling technique. With the progress in the development of computational technology, Computational Fluid Dynamics (CFD) is becoming the most available and useful tool for simulating a wide range of flow, mass, momentum and energy problems. The given set of axisymmetric conservation equations were solved computationally using the OLGA 7 flow assurance software via a finite element

approach. The consideration of the temperature trends by CFD simulation provides a useful tool for understanding the thermal behavior of CO<sub>2</sub> pipeline and finding optimum process parameters.

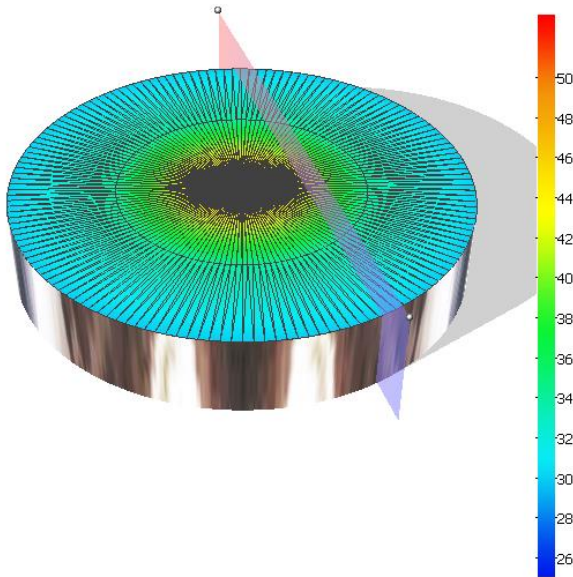


Figure 6 Temperature profile plotted by finite element analysis without insulation; summer case [Centigrade]

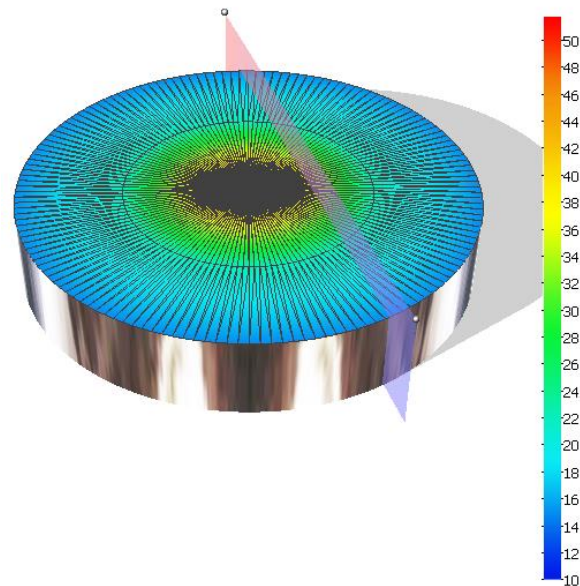


Figure 7 Temperature profile plotted by finite element analysis with insulation; winter case [Centigrade]

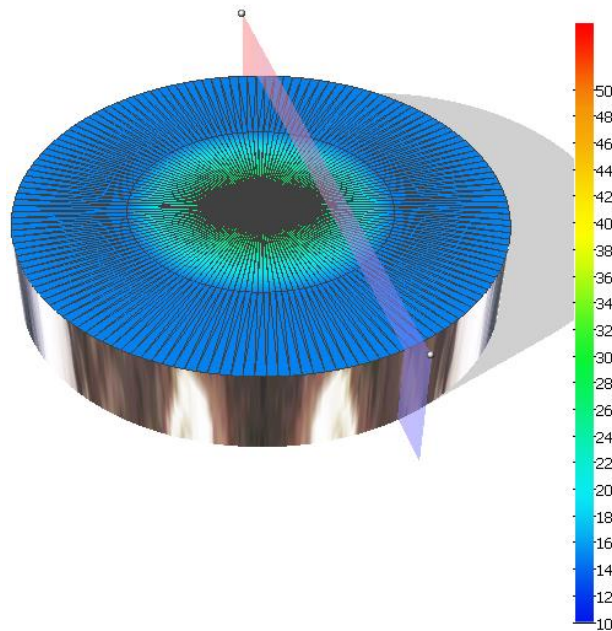


Figure 8 Temperature profile plotted by finite element analysis without insulation; winter case [Centigrade]

The mesh generated by OLGA simulator (fig. 4) consists of 527520 triangular cells and 510250 nodes. The temperature profile of CO<sub>2</sub> pipeline in the summer case is depicted in Figures 5 and 6 with and without insulation, respectively. Similar profiles have been illustrated in Figures 7 and 8 for the winter conditions. As the figures depict, in both summer and winter cases, insulation can help us to save more energy and prevent phase changing. Thus, chocking of the pipeline could be retarded and even removed by applying an appropriate insulation.

### 3.2. CO<sub>2</sub> pipeline hydraulic calculation

For the investigation of the pipeline hydraulic, the following assumptions have been considered. The transport flow rate was assigned to be 100 million ton CO<sub>2</sub>/year for a 40 km horizontal pipe line. The inlet conditions of CO<sub>2</sub> were assigned to be 17.6 MPa and 50°C (super-critical state). The flow velocity of CO<sub>2</sub> inside the pipeline is usually between 1-2 m/s, and an internal diameter of 0.15 m was considered based on trial calculation. The thickness of the thermal insulation layer was considered to be 25 mm. The slope angle of the pipeline was assumed to be zero, and the highest soil temperature is 35°C.

As concluded by other researchers [26-29], the pressure drop along the pipeline is dependent on the flow velocity, ambient temperature, the thermal insulation layer, as well as geometric characteristics of the pipeline such as length and elevation changes. The pressure drop along a 6 inch pipe diameter ( $k=0.738 \text{ W/m}^2\text{K}$ ) resulted from our simulation is sketched in fig.9. The pressure of the fluid decreases almost linearly along the pipeline because of friction. As the results illustrate, insulation has no effect on pressure profile of CO<sub>2</sub> transportation (two curves are the same). This effect has been concluded by Zhang *et al.* too [30]. Pressure drop along the pipeline is dominated by friction over the wall, and friction is dependent on CO<sub>2</sub> flow velocity and viscosity alike. Without insulation, temperature decreases more quickly, thus the CO<sub>2</sub> viscosity increases faster and pressure drop increases too. On the other hand, decreasing flow viscosity leads to the reduction of the fluid velocity, and consequently, the pressure drop decreases too. Eventually, these two conflicting effects cause no changes in pressure drop of CO<sub>2</sub> along the pipeline with or without insulation layer.

Figure 10 shows the pressure trend versus time in a specific point of the pipeline. As can be seen, it takes time to achieve the right pressure value in any point of the pipeline. For our conditions, this time was about 21 minutes for most of the pipe cross sections. It is due to the insulation layer causing the heat transferred to the medium to be a time-consuming process.

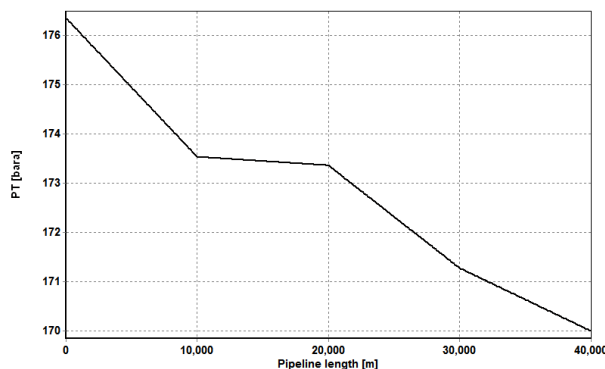


Figure 9 Pressure profile for 6 inch pipeline with and without insulation [bar]

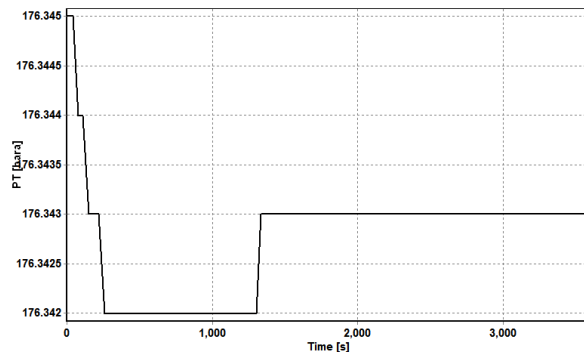


Figure 10 Pressure trend of CO<sub>2</sub> pipeline versus time [bar]

### 3.3. CO<sub>2</sub> pipeline thermal behavior

In reality, the properties of the soil such as heat capacity, thermal conductivity and diffusivity change over time since it alternately wets and dries. These quantities, which also differ along the pipeline, are difficult to predict. Therefore, tuning parameters of the model is required. The steady-state heat transfer neglects the response of the ground temperature as a result of heat accumulation. This assumption might cause larger temperature fluctuations in time due to the response of the soil resulting from heat accumulation. However, the insulation of the pipeline might mitigate this effect. Further investigation is required to examine to what extent these assumptions influence the results. The presence of impurities such as N<sub>2</sub>, H<sub>2</sub>, CO, H<sub>2</sub>O, SO<sub>2</sub>, NO<sub>2</sub>, and Ar were not included in the analysis. The temperature profile of CO<sub>2</sub> pipeline with and without insulation, in summer case, is depicted in Figures 11 and 12, respectively. Similar curves for winter conditions are also shown in Figures 13 and 14.

In the pipeline without insulation, CO<sub>2</sub> temperature approaches the soil temperature exponentially and finally reaches a level slightly above the soil temperature (30°C in summer and 15°C in winter). In this point, the decreasing trend of temperature due to Joule–Thomson effect almost offsets the increasing trend of temperature due to heat conduction from the soil to the CO<sub>2</sub> inside the pipe. After that, the CO<sub>2</sub> temperature stabilizes at this level, with very slight decreases along the pipeline.

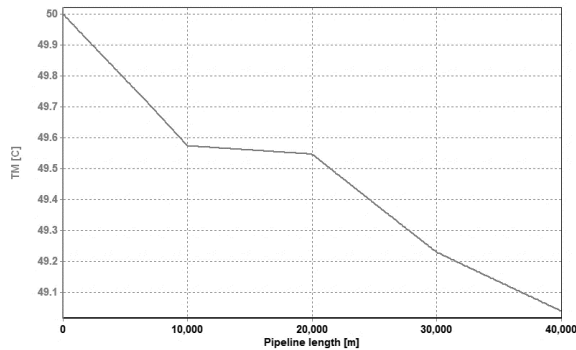


Figure 11 Temperature profile with insulation; summer case. [Centigrade]

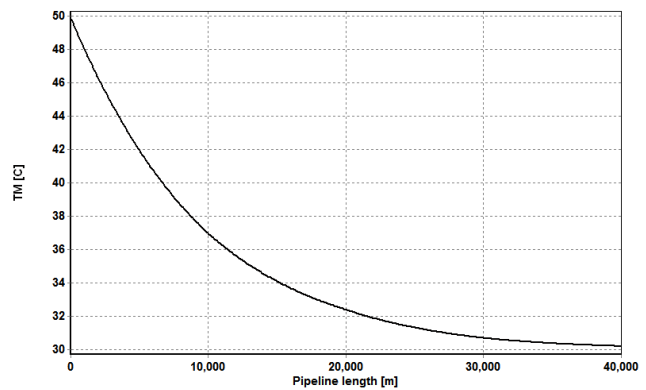


Figure 12 Temperature profile of CO<sub>2</sub> pipeline without insulation; summer case [Centigrade]

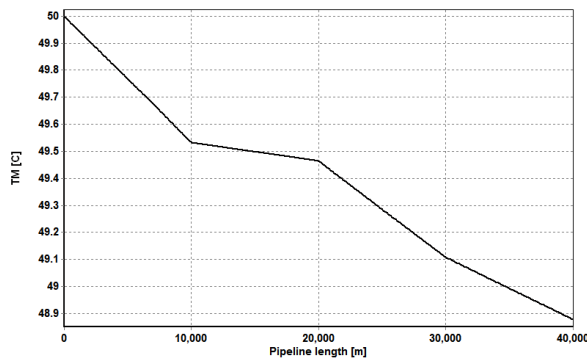


Figure 13 Temperature profile of CO<sub>2</sub> pipeline with insulation; winter case. [Centigrade]

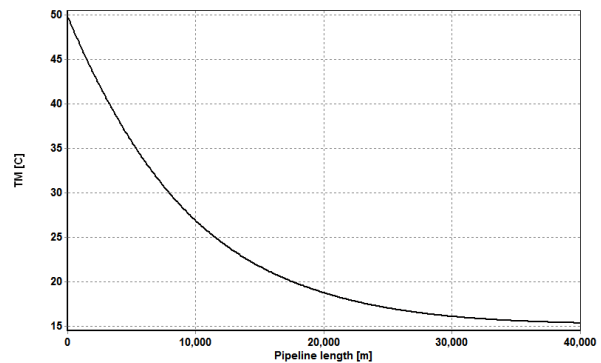


Figure 14 Temperature profile of CO<sub>2</sub> pipeline without insulation winter case. [Centigrade]

It can be seen that CO<sub>2</sub> temperature will drop quickly to a level above the soil temperature within a rather short distance and cause “pipe choking” due to violent vaporization. It should be cited that the vaporization happens more violently when no thermal insulation layer is applied, and the temperature also decreases faster, since more heat is transferred from soil to the CO<sub>2</sub>, exacerbating the vaporization process. However, as Figures 11 and 13 show, by using insulation, we can control the temperature and phase change of the CO<sub>2</sub>. The heat transfer coefficient between the fluid and the inner wall of the pipeline is demonstrated in Figure 15, which increases along the pipeline. The main reason behind this is the decrease in the temperature difference between the CO<sub>2</sub> and the medium.

To understand the impact of the pipe size, the pipeline operational parameters were calculated for different pipe size at the same ambient temperatures (Fig.16). In this case, we assume inlet temperature to the pipeline is 80 °C. It can be seen that CO<sub>2</sub> temperature decreases almost linearly along the pipeline due to heat transfer with the soil. The lower the pipe diameter, the more the pressure loss. And as a result, the more the pressure loss, the more temperature decrease. The reason is related to the pressure gradient.

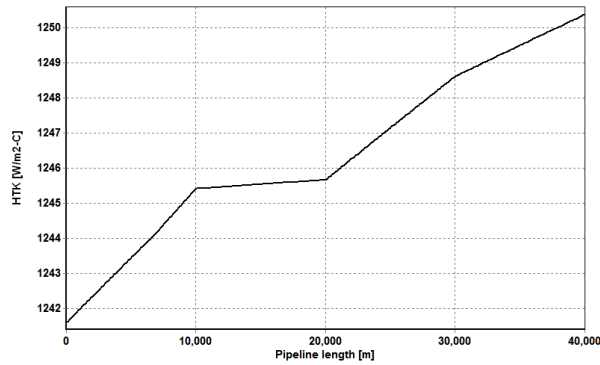


Figure 15 Heat transfer coefficient of inner wall with insulation. [ $W/m^2.C$ ]

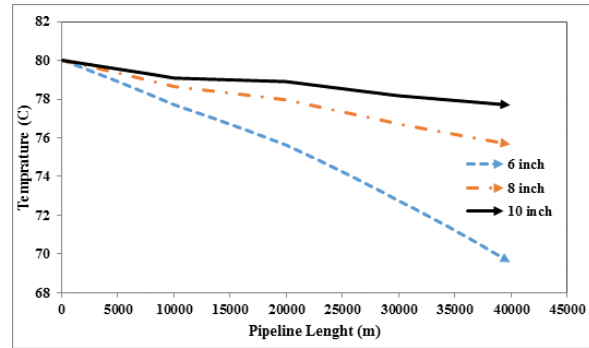


Figure 16 Temperature profile in different pipe size. [Centigrade]

#### 4. Conclusion

This paper studied the effect of factors such as the ambient temperature and the thermal insulation layer on the thermodynamic properties of the  $CO_2$  flow in the pipeline and its thermal behavior. We built a one-dimension static flow model for  $CO_2$  pipeline and studied the hydrodynamic performance of  $CO_2$  flow in the pipeline, as well as the impacts of multiple factors, including pipe diameter and soil temperature. It proposes certain principles concerning the design of  $CO_2$  transport pipelines and the determination of their hydraulic parameters with the thermal insulation layer to ensure a minimum pressure drop in harsh Iranian climate. As can be seen, insulation layer should be considered for transporting  $CO_2$  in supercritical state. Additionally, to reduce capital cost, it is better to have less pressure and temperature losses. The size of the pipeline could also assist us to justify the losses. Therefore, the diameter of the pipe line should be considered too. In the simulation process, the time that the parameters take to reach the stable value should be taken into account too. This study was conducted based upon this assumption that the pipeline lies horizontally over the whole distance. In reality, however, the pipeline will inevitably face topographical slopes in the midway, such as the cases of climbing mountainous or hilly districts, so the impacts of elevation should be studied in detail.

#### Nomenclature

$A^f, A, A^w$	Area of the pipe cross section, $m^2$
$T^f, T, T_s, T^w$	Temperature, K
$\rho^f, \rho, \rho^w$	Density, $kg/m^3$
$C_p^f, C_p, C_p^w$	Heat capacity, $J/kg.K$
$m$	Flow rate of fluid
$C_p^f, C_p, C_p^w$	Heat transfer, $J/sec.area$
$\lambda, k_{soil}, k_{in}$	Conductivity, $W/m^2.K$
$\vec{j}_q$	Heat flux, $W/m^2$
$\vec{n}$	Unit outward normal at the FEM domain boundary
$p$	Pressure, pa
$T$	Time, sec
$V$	Velocity, $m/s$
$x$	Spatial coordinate, $m$
$a_s$	Isentropic wave speed, $m/s$
$z$	Distance, $m$
$w$	Frictional force per unit length, $N/m$
$g$	Gravitational acceleration, $m/s^2$
$\theta$	Inclination angle of pipe, radian
$d$	Pipeline diameter, $m$
$f$	Friction factor

$\varepsilon$	<i>Pipe roughness, m</i>
$r_1$	<i>Inner pipeline radius, m</i>
$r_2$	<i>Outer pipeline radius with insulation, m</i>
$h_g$	<i>Convective heat transfer, <math>W/m^2K</math></i>

## References

- [1] Petukhov B. Advances in heat transfer. 1970; 6: i565.
- [2] Hall W, Jackson J. Advances in Heat Transfer. 1971, 7, 86.
- [3] Jackson J, Hall W, Fewster J, Watson A, Watts M. Heat transfer to Supercritical Pressure Fluids, U. K. A. E. A. E. R. E.-R 8158, Design Report 34, 1975.
- [4] Shitsman M. High temperature. 1963; 1(2): 237-244.
- [5] Krasnoshchekov E, Protopopov V. High Temperature. 1966; 4(3): 375-382.
- [6] Yamagata K, Nishikawa K, Hasegawa S, Fujii, T, Yoshida S. International Journal of Heat and Mass Transfer. 1972; 15(12): 2575-2593.
- [7] Petukhov B, Krasnoshchekov E, Protopopov V. An investigation of heat transfer to fluids flowing in pipes under supercritical conditions; ASME International Developments in Heat Transfer Part 3, 1961.
- [8] Watts M, Chou C. Mixed convection heat transfer to supercritical pressure water; Proceedings of the 7th International Heat Transfer Conference, 1982.
- [9] Hassan SN, Douglas PL, Croiset E. International Journal of green energy. 2007; 4: 197-220.
- [10] Giuffrida A, Romano MC, Lozza G. CO<sub>2</sub> capture from air-blown gasification-based combined cycles; ASME Turbo Expo 2012: Turbine Technical Conference and Exposition; American Society of Mechanical Engineers, 2012.
- [11] Barker D, Turner S, Napier-Moore P, Clark M, Davison J. Energy Procedia. 2009; 1(1): 87-94.
- [12] Johansson D, Franck PÅ, Berntsson T. Energy Conversion and Management. 2013; 66: 127-142.
- [13] Davidson O, de Coninck H, Loos M, Meys, L. IPCC Special Report on Carbon Dioxide Capture and Storage, Prepared by Working Group III of the Intergovernmental Panel on Climate Change; Cambridge University Press, 2005.
- [14] Svensson R, Odenberger M, Johnsson F, Strömberg L. Energy Conversion and Management. 2004; 45(15): 2343-2353.
- [15] Uilhoorn FE. International Journal of Greenhouse Gas Control. 2013; 14(5): 177-182.
- [16] Vandeginste V, Piessens K. International Journal of Greenhouse Gas Control. 2008; 2(4): 571-581.
- [17] S J. Flow assurance of deepwater oil and gas production: a review, ASME 2003 22<sup>nd</sup> International Conference on Offshore Mechanics and Arctic Engineering; American Society of Mechanical Engineers, 2003.
- [18] Palmer A, White D, Baumgard A, Bolton M, Barefoot A, Finch M. Uplift resistance of buried submarine pipelines: comparison between centrifuge modelling and full-scale tests; THOMAS TELFORD PUBLISHING THOMAS TELFORD HOUSE, 2005.
- [19] Zhang Z, Wang G, Massarotto P, Rudolph V. Energy Conversion and Management. 2006; 47: 702-715.
- [20] McCoy ST, Rubin ES. International Journal of Greenhouse Gas Control. 2008; 2(2): 219-229.
- [21] Forbes SM, Verma P, Curry TE, Friedmann SJ, Wade S. Guidelines for carbon dioxide capture, transport and storage; World Resources Institute, 2008.
- [22] Thorley A, Tiley C. International journal of heat and fluid flow. 1987; 8(1): 3-15.
- [23] Colebrook CF. Journal of the ICE. 1939; 11(4): 133-156.
- [24] Bozzoli F, Pagliarini G, Rainieri S, Schiavi L. Energy. 2011; 36(2): 839-846.
- [25] Bøhm B. International journal of energy research. 2000; 24(15): 1311-1334.
- [26] Barletta A, Lazzari S, Zanchini E, Terenzi A. Heat Transfer Engineering. 2008; 29(11): 942-949.
- [27] Xu C, Yu B, Zhang Z, Zhang J, Wei J, Sun S. Petroleum Science. 2010; 7(1): 73-82.
- [28] Bai Y, Niedzwecki JM. Computers and Geotechnics. 2014; 61: 221-229.
- [29] Verda V, Colella F. Energy. 2011; 36(7): 4278-4286.
- [30] Dongjie Z, Zhe W, Jining S, Lili Z, Zheng L. Energy Conversion and Management. 2012; 55: 127-135.

To whom correspondence should be addressed. E-mail: [abbas.azarmehr.put@gmail.com](mailto:abbas.azarmehr.put@gmail.com)